An International Journal
computers & mathematics with applications

PERGAMON Computers and Mathematics with Applications 40 (2000) 589–605

www.elsevier.nl/locate/camwa

Maxwell Eigenvalues and Discrete Compactness in Two Dimensions

L. DEMKOWICZ, P. MONK, CH. SCHWAB AND L. VARDAPETYAN
Texas Institute for Computational and Applied Mathematics
The University of Texas at Austin
Austin, TX 78712, U.S.A.

(Received and accepted October 1999)

Abstract—We present an elementary proof of the discrete compactness result for a general class of *hp* finite elements introduced in [1,2]. We discuss *h*-convergence of 2D elements only, and in this context, the results are not new as the analysis of $H(\mathrm{curl})$-conforming elements for Maxwell's equations can be reduced to the long-known results for Raviart-Thomas elements [3]. The work is based on the result of Kikuchi [4,5] for Nedelec's edge triangular elements of the lowest order and presents an alternative to techniques presented in [3,6]. In particular, the present version does not use an inverse inequality argument, and therefore, is valid for *h*-adaptive meshes. We conclude the presentation with a number of 2D computational experiments, including nonconvex domains.

Keywords—Maxwell's equations, *hp* finite elements.

1. INTRODUCTION

Eigenvalue problems for Maxwell's equations have a number of useful applications including the design of microwave resonators, microwave ovens, and communication equipment, see, e.g., [4,7,8]. In addition, if an error estimate is available for the eigenvalue problem, it is possible to prove the discrete Babuška-Brezzi condition for the corresponding source problem, and hence, obtain an optimal error estimate [1,2,6].

The basic problem is, given a bounded domain $\Omega \subset \mathbb{R}^N$, $N = 2, 3$, to find a field $\mathbf{E} \neq \mathbf{0}$, and a constant $\lambda > 0$ such that

$$\begin{aligned} \nabla \times \nabla = \lambda \mathbf{E}, &\qquad \text{in } \Omega, \\ \mathbf{n} \times \mathbf{E} = \mathbf{0}, &\qquad \text{on } \Gamma := \partial\Omega. \end{aligned} \tag{1.1}$$

In addition to be physically realistic, the eigenvectors must satisfy

$$\nabla \circ \mathbf{E} = 0, \qquad \text{in } \Omega. \tag{1.2}$$

Notice that the divergence condition is automatically satisfied provided $\lambda \neq 0$ and we shall only be interested in computing nonzero eigenvalues here (the eigenfunctions corresponding to $\lambda = 0$ can be easily characterized and computed—see [7]).

The work of L. Demkowicz and L. Vardapetyan has been supported by the Air Force under Contract F49620-98-1-0255. The work of P. Monk has been supported by the Air Force under Contract F49620-98-1-0019.

0898-1221/00/$ - see front matter Typeset by $\mathcal{A}\mathcal{M}\mathcal{S}$-TEX
PII: S0898-1221(00)00182-6

To discretize the eigenvalue problem, we need a variational formulation of the original problem [9,10]. Let

$$\mathbf{H}_0(\mathrm{curl};\Omega) = \left\{\mathbf{E} \in \mathbf{L}^2(\Omega) : \nabla \times \mathbf{E} \in \mathbf{L}^2(\Omega), \mathbf{n} \times \mathbf{E} = \mathbf{0} \text{ on } \Gamma\right\}, \tag{1.3}$$

and let

$$(\mathbf{E}, \mathbf{F}) = \int_\Omega \mathbf{E} \circ \bar{\mathbf{F}}\, d\mathbf{x}. \tag{1.4}$$

Then the variational problem is to find $\mathbf{E} \in \mathbf{H}_0(\mathrm{curl} : \Omega), \mathbf{E} \neq \mathbf{0}$, and $\lambda \neq 0$ such that

$$(\nabla \times \mathbf{E}, \nabla \times \mathbf{F}) = \lambda(\mathbf{E}, \mathbf{F}), \qquad \forall \mathbf{F} \in \mathbf{H}_0(\mathrm{curl};\Omega). \tag{1.5}$$

Again the divergence condition is automatically satisfied. We can see this by noting that if $q \in H_0^1(\Omega)$, then $\nabla q \in \mathbf{H}_0(\mathrm{curl};\Omega)$ and using $\mathbf{F} = \nabla q$ in (1.5) shows that

$$(\mathbf{E}, \nabla q) = 0, \qquad \forall q \in H_0^1(\Omega). \tag{1.6}$$

This is a variational enforcement of the divergence condition.

To discretize the problem, we construct a finite element approximation space $\mathbf{W}_h \subset \mathbf{H}_0(\mathrm{curl};\Omega)$ and compute $\mathbf{E}_h \in \mathbf{W}_h, \mathbf{E}_h \neq \mathbf{0}$ and $\lambda_h \neq 0$ such that

$$(\nabla \times \mathbf{E}_h, \nabla \times \mathbf{F}_h) = \lambda_h(\mathbf{E}_h, \mathbf{F}_h), \qquad \forall \mathbf{F}_h \in \mathbf{W}_h. \tag{1.7}$$

It is well known that the use of standard continuous finite elements to construct $\mathbf{W}_h$ results in spurious eigenvalues. These can be eliminated by adding a term to control the divergence of the field to the variational problem [4], but the method will not converge on nonconvex polygonal or polyhedral domains unless singularities in the solution are taken into account, see the discussion in [11]. An alternative used frequently in practice is to use the edge elements of Nédélec [12,13][1]. In this paper, we shall examine the use of a new family of *hp* elements introduced in [1,2] (see also [14]), that generalize Nédélec's triangles (tetrahedra) of the second kind, and Nédélec's quads (hexahedra) of the first kind.

For the edge elements we shall consider here, there is a space of scalar functions $V_{0,h} \subset H_0^1(\Omega)$ such that

$$\nabla V_{0,h} = \mathbf{W}_h \cap \mathcal{N}(\nabla\times), \tag{1.8}$$

where $\mathcal{N}(\nabla\times)$ denotes the null space of the curl operator defined on $\mathbf{H}_0(\mathrm{curl};\Omega)$, and $\mathbf{W}_h$ stands for the finite element space corresponding to the *hp* elements. In other words, the following compatibility condition holds.

$$\nabla \times \mathbf{E}_h = \mathbf{0}, \mathbf{E}_h \in \mathbf{W}_h, \qquad \text{if and only if } \exists q_h \in V_h, \mathbf{E}_h = \nabla q_h. \tag{1.9}$$

As usual, we skip *p*—the symbol for possibly *locally varied* order of approximation, in the notation for the discrete solutions and spaces.

Choosing the test function $\mathbf{F}_h = \nabla q_h$, $q_h \in V_h$, we see that, provided $\lambda_h \neq 0$, the following discrete divergence condition is satisfied by the approximate eigenfield (compare to (1.6)).

$$(\mathbf{E}_h, \nabla q_h) = 0, \qquad \forall q_h \in V_{0,h}. \tag{1.10}$$

Until recently, the proof of convergence of Maxwell eigenvalues in 3D was limited to the case of the lowest-order Nédélec edge elements of the second kind on tetrahedra. The proof, given by Kikuchi [4,5] (see also a related analysis for 2D wave guide eigenvalue problems in [8]) involved the verification of a discrete compactness result. Unfortunately, the key estimate involved in

[1] We shall refer to elements from [12] and [13] as the Nédélec elements of the *first* or the *second kind*, respectively.

this proof does not hold for elements of higher order or elements on quads. The existing proof guarantees convergence (without an order estimate) on arbitrary Lipschitz domains. When the eigenfunctions are smooth, an order estimate can be proved using the work of Mercier, Osborn *et al.* [15] on eigenvalues of collectively compact operators (see [8] for 2D wave-guide problems). We remark that an attempt to use the mixed finite element theory given in [7] unfortunately fails since the proof that the discrete operators converge to the continuous operator in norm is mistaken.

A new approach has been recently presented in a series of papers by Boffi *et al.* (see [3,16] and the literature therein). The proposed technique is based on a construction of the Fortin operator and applies to Nedelec's tetrahedral elements of arbitrary order, and among others, arbitrary polyhedral domains. The construction is based on the de Rham diagram that holds for Nedelec and Raviart-Thomas spaces, and has recently been extended for the *hp*-spaces as well [17].

In [6], we used the theory of collectively compact operators to prove *h*-convergence for both source and eigenvalue problems for general edge elements in both 2D and 3D. The proof is based on an extension of the Kikuchi's discrete compactness argument to edge elements of arbitrary order. In the work, however, we used an inverse inequality argument, eliminating the use of general *h*-adaptive meshes[2]. In this note, we present an alternative, elementary proof of the discrete compactness result that avoids using the inverse inequality and applies to arbitrary 2D meshes.

The Eigenvalue Problem in $\mathbb{R}^2$

The most interesting class of eigenvalue problems in $\mathbb{R}^2$ arises from computing wave-guide modes [8,18]. This is a complicated problem in its own right, and we defer an analysis of problems of this type until a later paper. Instead, here we consider only the 2D version of the problem discussed above. We first recall the definition of the *hp* elements on triangles and quads. Next we state and prove the discrete compactness result for the *h* version of the *hp* elements that is the main theoretical contribution of this paper. Using this, we can then verify the *h*-convergence of the discrete eigenvalue problem for elements of *arbitrary, possibly variable, but limited* order of approximation p.

2. THE *hp* ELEMENTS

The key to the construction of the elements is the compatibility condition (1.9) that mimics an analogous compatibility condition satisfied at the continuous level.

2.1. Triangular Master Element

The element occupies the standard unit right triangle illustrated in Figure 1. It has seven nodes: three vertex nodes $\hat{\mathbf{a}}_i$, $i = 1,2,3$, three mid-edge nodes $\hat{\mathbf{a}}_i$, $i = 4,5,6$, and the middle node $\hat{\mathbf{a}}_7$. The element space of scalar-valued shape functions $V_h(\hat{K})$ is standard [19], and it consists of polynomials of order $p+1$ whose restrictions to element edges $\hat{e}_i$ reduce to polynomials of order $p_i + 1$,

$$V_h\left(\hat{K}\right) = \left\{\hat{u} \in \mathcal{P}^p\left(\hat{K}\right) : \hat{u}|_{\hat{e}_i} \in \mathcal{P}^{p_i+1}(\hat{e}_i),\ i = 1,2,3\right\}, \tag{2.11}$$

where we assume that

$$p_1, p_2, p_3 \leq p. \tag{2.12}$$

Take now a function $q \in V_h(\hat{K})$. In general, when differentiating a polynomial of order $p+1$, we obtain another polynomial of order p. In the case, however, of a directional derivative taken along the i^{th} element edge, where the restriction of function q is of a lower order $p_i + 1$, the

[2]In particular geometrically graded meshes essential for modeling singularities.

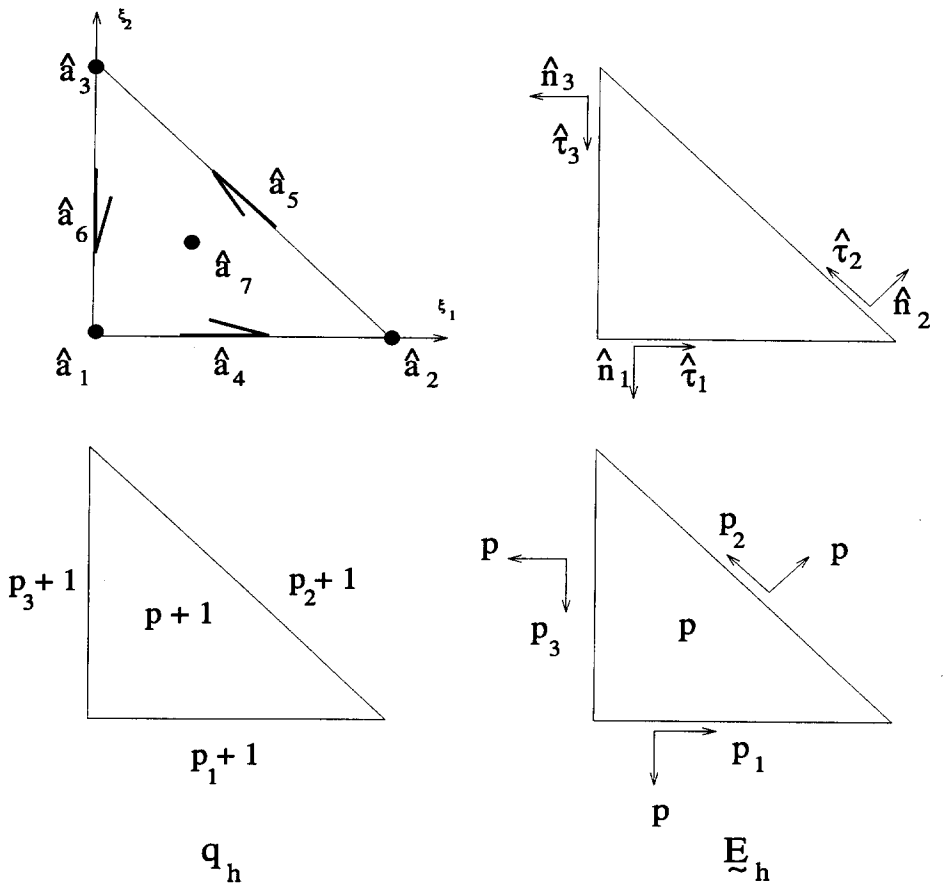

Figure 1. Triangular master element for Maxwell's equations.

differentiation will give us a polynomial only of order p_i. This leads to the following definition of the element space of shape functions $\mathbf{W}_h(\hat{K})$ for the electric field:

$$\mathbf{W}_h\left(\hat{K}\right) = \left\{\hat{\mathbf{E}} \in \mathbf{P}^p\left(\hat{K}\right) : \hat{\mathbf{E}}\Big|_{\hat{e}_i} \cdot \hat{\tau}_i \in \mathcal{P}^{p_i}\left(\hat{e}_i\right),\ i = 1,2,3\right\}, \tag{2.13}$$

where $\hat{\tau}_i$, $i = 1,2,3$ are tangent vectors to the element edges. Notice that the normal components of the **E**-field on the boundary are, in general, of order p. This does not pose problems in connecting elements of different order in the mesh as long as the *minimum rule* is used [19].

The choice of concrete shape functions is, from the point of view of this analysis, arbitrary. In practice it does affect, of course, the conditioning of the final matrices. Referring to [14] for an example of an implementation involving hierarchical shape functions, we shall make the following assumptions.

Scalar-valued shape functions are classified into three groups.

- Vertex linear shape functions,

$$\hat{\psi}^v_1 = 1 - \xi_1 - \xi_2, \qquad \hat{\psi}^v_2 = \xi_1, \qquad \hat{\psi}^v_3 = \xi_2. \tag{2.14}$$

- Mid-edge nodes shape functions,

$$\hat{\psi}^e_{i,j}, \qquad j = 1,\ldots,p_i, \quad i = 1,2,3, \tag{2.15}$$

that vanish on edges $i+1$, $i+2$ (modulo 3), and their restrictions to the i^{th} edge span polynomials of order $p_i + 1$.

- Middle node shape functions,

$$\hat{\psi}_j^m, \qquad j = (p-1)\frac{p}{2}, \tag{2.16}$$

that vanish on the boundary of the element.

Vector-valued shape functions are classified into two groups.

- Mid-edge nodes shape functions,

$$\hat{\psi}_{i,j}^e, \qquad j = 1, \ldots, p_i + 1, \quad i = 1, 2, 3, \tag{2.17}$$

that vanish on edges $i+1$, $i+2$ (modulo 3), and the restrictions of their tangential components to the i^{th} edge span polynomials of order p_i.

- Middle node shape functions,

$$\hat{\psi}_j^m, \qquad j = 1, \ldots, 3(p-1) + (p-2)(p-1), \tag{2.18}$$

whose tangential components vanish on the element boundary. They include $(p-2)(p-1)$ shape functions vanishing completely on the boundary, and $3(p-1)$ functions with a nonzero normal component on the boundary.

The definition applies to $p > 1$. The lowest (zero) order element is defined differently. The space of the element scalar-valued shape functions consists of linear polynomials, but the space of the vector-valued shape functions-W_h consists of functions of the form

$$\begin{pmatrix} a \\ b \end{pmatrix} + c \begin{pmatrix} -y \\ x \end{pmatrix}. \tag{2.19}$$

2.2. Quadrilateral Master Element

The element occupies the standard unit square illustrated in Figure 2. It has nine nodes: four vertex nodes $\hat{a}_i, i = 1, \ldots, 4$, four mid-edge nodes $\hat{a}_i, i = 5, \ldots, 8$ and the middle node $\hat{a}_9$.

The element space of scalar-valued shape functions $V_h(\hat{K})$ consists of polynomials of order $(p_h + 1, p_v + 1)$ whose restrictions to element edges $\hat{e}_i$ reduce to polynomials of order $p_i + 1$, $i = 1, \ldots, 4$,

$$V_h\left(\hat{K}\right) = \left\{\hat{u} \in \mathcal{Q}^{(p_h+1, p_v+1)}\left(\hat{K}\right) : \hat{u}|_{\hat{e}_i} \in \mathcal{P}^{p_i+1}\left(\hat{e}_i\right),\ i = 1, \ldots, 4\right\}, \tag{2.20}$$

where we assume that

$$p_1, p_3 \leq p_h, \qquad p_2, p_4 \leq p_v. \tag{2.21}$$

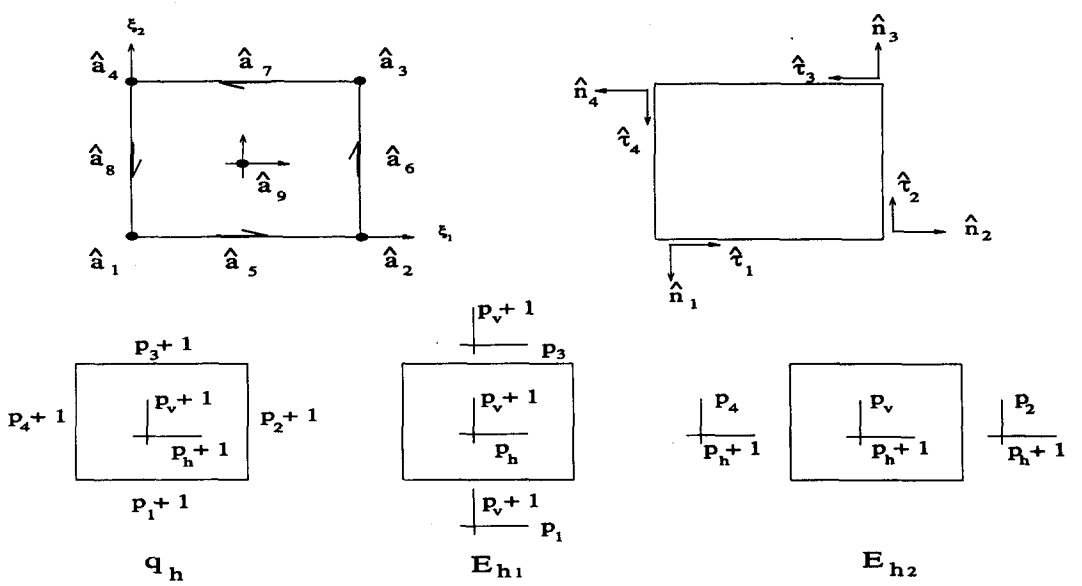

Figure 2. Quadrilateral master element for Maxwell's equations.

As in the case of the triangular element, the shape functions can be grouped as follows:

- bilinear shape functions associated with the vertices

$$\hat{\phi}_i^v, \qquad i = 1,2,3,4; \tag{2.22}$$

- p_i shape functions associated with the edges $\hat{e}_i$, $i = 1,2,3,4$

$$\hat{\phi}_{i,j}^e, \qquad j = 1,\ldots,p_i; \tag{2.23}$$

- the shape functions associated with the middle node

$$\hat{\phi}_{5,j}^m, \qquad j = 1,\ldots,p_h p_v. \tag{2.24}$$

The reasoning in introducing the vector-valued shape functions is essentially the same as for the triangle, and it is based on the discrete compatibility condition (1.9). Given an arbitrary polynomial $q(x_1,x_2)$ from the space of the scalar shape functions, we calculate its gradient to figure out the right space for the approximation of the **E**-field. The concept is illustrated in Figure 3. First of all, the corresponding orders of approximation for the components are different, we have polynomials of order (p_h, p_v+1) for the horizontal component, and polynomials of order (p_h+1, p_v) for the vertical one. Second, the order of approximation for the normal component along the boundary, i.e., the first component for the second and fourth edges, and the second component for the first and third edges, does not longer depend only upon the order of approximation for the middle node only. This is inconsistent with the logic for the triangles where the normal edge shape functions have been assigned to the middle node and are characterized by the middle node order of approximation only. For that reason, we enlarge slightly the spaces, and define the corresponding space of vector-valued shape functions as follows:

$$\mathbf{W}_h\left(\hat{K}\right) = \left\{(E_1,E_2): \begin{array}{l} E_1 \in \mathcal{Q}^{p_h,p_v+1}, \text{ such that } E_1(\cdot,0) \in \mathcal{P}^{p_1},\ E_1(\cdot,1) \in \mathcal{P}^{p_3} \\ E_2 \in \mathcal{Q}^{p_h+1,p_v}, \text{ such that } E_2(1,\cdot) \in \mathcal{P}^{p_2},\ E_2(0,\cdot) \in \mathcal{P}^{p_4} \end{array}\right\}. \tag{2.25}$$

Note that the slight increase of the space compared with the range of the gradient operator *does not* violate the compatibility condition (1.9).

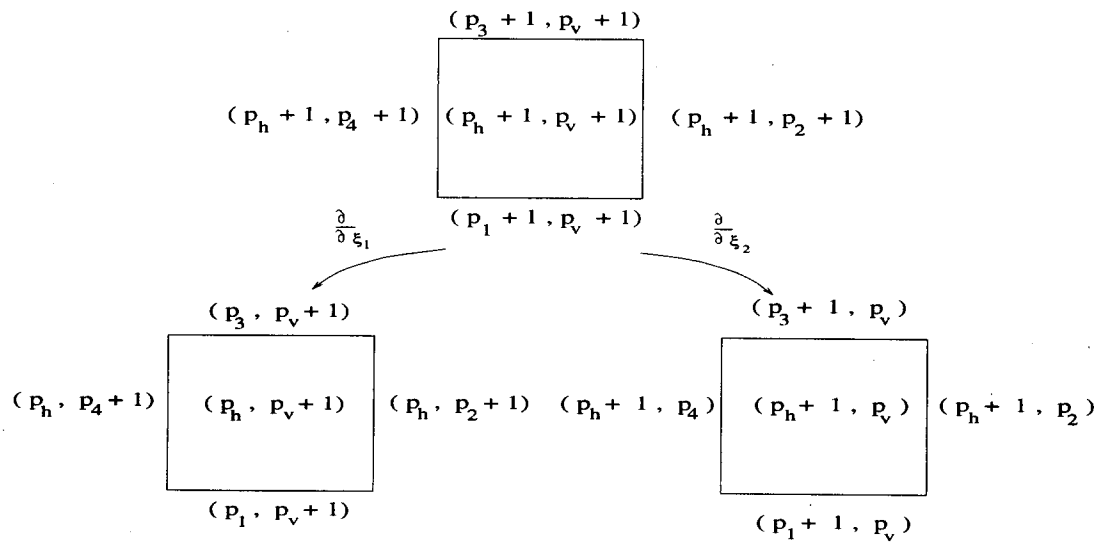

Figure 3. Orders of approximation for the gradient of a scalar shape function.

Denoting by $\hat{\tau}_i, \hat{\mathbf{n}}_i$, $i = 1, \ldots, 4$ the unit tangential and normal vectors for the element edges, comp. Figure 2, we introduce the vector-valued shape functions as follows.

- For each mid-side node $\hat{\mathbf{a}}_{4+i}, i = 1, \ldots, 4$, we have a total of p_i+1 shape functions including two linear shape functions,

$$\hat{\tau}_i \hat{\phi}_i, \qquad \hat{\tau}_i \hat{\phi}_{i+1}, \tag{2.26}$$

and $p_i - 1$ higher-order shape functions,

$$\hat{\tau}_i \hat{\phi}_{i,j}, \qquad j = 1, \ldots, p_i - 1. \tag{2.27}$$

- The middle node groups normal edge shape functions, ordered edge-wise,

$$\hat{\mathbf{n}}_i \hat{\phi}_{i,j}, \qquad j = 1, \ldots, p - 1, \tag{2.28}$$

with $p = p_h$ for the first and third edge, and $p = p_v$ for the second and third edge, and the shape functions vanishing on the boundary:

- $(p_h - 1)p_v$ shape functions for the horizontal component:

$$(1,0)\ \hat{\chi}_k(\xi_1)\hat{\chi}_l(\xi_2), \qquad k = 3, \ldots, p_h + 1, \quad l = 3, \ldots, p_v + 2; \tag{2.29}$$

- $p_h(p_v - 1)$ shape functions for the vertical component:

$$(0,1)\ \hat{\chi}_k(\xi_1)\hat{\chi}_l(\xi_2), \qquad k = 3, \ldots, p_h + 2, \quad l = 3, \ldots, p_v + 1. \tag{2.30}$$

Here $\hat{\chi}_j$ denote one-dimensional shape functions vanishing at the element endpoints. For the lowest, 0^{th}-order elements, space V_h consists of bilinear functions only and the tangential components of the mid-edge vector-valued shape functions are constant. In other words, we have

$$\hat{E}_1 = a_1(1 - \xi_2) + a_3\xi_2, \qquad \hat{E}_2 = a_4(1 - \xi_1) + a_2\xi_1, \tag{2.31}$$

where $a_1, \ldots, a_4$ are the values of the constant tangential components along the four edges.

2.3. Parametric Element

We use the standard procedure to define parametric (deformed) quads and triangles for the scalar-valued functions. Given a bijective map

$$\mathbf{x}_K : \hat{K} \to K \tag{2.32}$$

from either master quad or triangle onto an element K, we define the element space of shape functions as the collection of compositions of inverse $\mathbf{x}_K^{-1}$ and the master element shape functions,

$$V_h(K) = \left\{ u = \hat{u} \circ \mathbf{x}_K^{-1} : \hat{u} \in V_h\left(\hat{K}\right) \right\}. \tag{2.33}$$

Accordingly, the element scalar shape functions are defined as

$$\phi_i(\mathbf{x}) = \hat{\phi}_i(\boldsymbol{\xi}), \qquad \text{where } \mathbf{x}_K(\boldsymbol{\xi}) = \mathbf{x}. \tag{2.34}$$

For each element K, we shall speak about its vertex, mid-edge, and middle nodes, understood again simply as an abstraction for the element vertices, edges, and interior.

The definition of the parametric approximation for the vector-valued functions is more elaborate. The key lies again in the compatibility condition (1.9) which implies that, when passing

to the deformed element, the vector field must transform the same way as the gradients of the scalar fields. That is,

$$\frac{\partial q}{\partial x_i} = \sum_{j=1}^{2} \frac{\partial \hat{q}}{\partial \xi_j} \frac{\partial \xi_j}{\partial x_i} \tag{2.35}$$

implies that

$$E_i(\mathbf{x}) = \sum_{j=1}^{2} \hat{E}_j(\boldsymbol{\xi}) \frac{\partial \xi_j}{\partial x_i}(\boldsymbol{\xi}), \qquad \text{where } \mathbf{x} = \mathbf{x}_K(\boldsymbol{\xi}). \tag{2.36}$$

In particular, the element shape functions are defined as

$$\boldsymbol{\psi}_i = (\psi_{i,j}), j = 1,2, \qquad \psi_{i,j}(\mathbf{x}) = \sum_{l=1}^{2} \hat{\psi}_{i,l}(\boldsymbol{\xi}) \frac{\partial \xi_l}{\partial x_j}(\mathbf{x}). \tag{2.37}$$

Values of the tangent components of the field on the actual and master elements can be related as follows:

$$\mathbf{E} \cdot \frac{d\mathbf{r}}{ds} = \hat{E}_j \frac{\partial \xi_j}{\partial x_i} \frac{dx_i}{ds} = \hat{E}_j \frac{d\xi_j}{ds} = \hat{E}_j \frac{d\xi_j}{d\zeta} \left(\frac{ds}{d\zeta}\right)^{-1}, \tag{2.38}$$

where $\frac{d\mathbf{r}}{ds}$ is a unit tangent vector, $\mathbf{r} = \mathbf{r}(s)$ denotes the parameterization of the element side with the natural parameter s, $\boldsymbol{\xi}(s)$ and $\boldsymbol{\xi}(\zeta)$ are the corresponding parameterizations of the master element side. Consequently, for standard meshes, the continuity of the tangential component is enforced on the master element level by matching the corresponding d.o.f. for the mid-edge shape functions. For meshes resulting from h-refinements, the constrained approximation must be used [14].

In the presented analysis, we shall restrict ourselves to regular affine meshes only. By the regularity we mean that, for each element K,

$$\frac{h_K}{\rho_K} \leq \sigma, \tag{2.39}$$

where h_K is the diameter of K, ρ_K is the diameter of the largest inscribed circle contained in K, and σ is mesh independent.

REMARK 1. Note the transformation rule for the curl operator when switching from the master to the current element:

$$\nabla \times \boldsymbol{\psi} = \frac{\nabla_{\boldsymbol{\xi}} \times \hat{\boldsymbol{\psi}}}{J}, \tag{2.40}$$

where J is the Jacobian of transformation $\mathbf{x}_K$. In particular, for the affine elements of the lowest order, both triangles and quads, $\operatorname{curl} \mathbf{E}_h = \text{const}$. From the corresponding transformation rule for the divergence,

$$\sum_{i=1}^{2} \frac{\partial E_i}{\partial x_i} = \sum_{j=1}^{2} \sum_{l=1}^{2} \sum_{i=1}^{2} \frac{\partial \hat{E}_j}{\partial \xi_l} \frac{\partial \xi_l}{\partial x_i} \frac{\partial \xi_j}{\partial x_i}. \tag{2.41}$$

We can see the difference between the lowest, 0^{th}-order affine triangles and quads. Whereas for the triangles the divergence is always zero, for quads it is zero only when the factor

$$\sum_{i=1}^{2} \frac{\partial \xi_1}{\partial x_i} \frac{\partial \xi_2}{\partial x_i} \tag{2.42}$$

vanishes. This is the case for rectangular elements only. ∎

3. DISCRETE COMPACTNESS

Denote

$$\begin{aligned} X_N &:= H_0(\mathrm{curl};\Omega) \cap H(\mathrm{div};\Omega), \\ H^1_N &:= X_N \cap H^1(\Omega). \end{aligned} \tag{3.43}$$

We begin by recalling the *comparison theorem*, see e.g., [20, Theorem 2.2].

THEOREM 1. *Any* $\mathbf{E} \in X_N$ *has a continuous decomposition*

$$\mathbf{E} = \mathbf{E}^* + \nabla\phi, \qquad \text{with} \begin{cases} \mathbf{E}^* \in H^1_N(\Omega), \\ \phi \in H^1_0(\Omega), \qquad \Delta\phi \in L^2(\Omega). \end{cases} \tag{3.44}$$

COROLLARY. *It follows from the standard regularity theory for the Laplace equation that, for Lipschitz or polyhedral domains* $\Omega \subset \mathbb{R}^2$, X_N *is continuously imbedded in* $H^{1/2-\epsilon}(\Omega)$ *with any* $\epsilon > 0$. *Consequently,* X_N *is compactly imbedded in* $L^2(\Omega)$.

We can restate now Kikuchi's result [5].

THEOREM 2. *Let* $\mathbf{E}^0_h$ *be a sequence of fields corresponding to the zero order triangular elements such that*

- $\mathbf{E}^0_h$ *is uniformly bounded in the* $\mathbf{H}(\mathrm{curl},\Omega)$*-norm,*

$$\left\|\mathbf{E}^0_h\right\|^2 + \left\|\nabla \times \mathbf{E}^0_h\right\|^2 \leq 1, \qquad \forall h; \tag{3.45}$$

- $\mathbf{E}^0_h$ *are discrete divergence-free,*

$$\left(\mathbf{E}^0_h, \nabla q_h\right) = 0, \qquad \forall q_h \in V_h. \tag{3.46}$$

Then there exists a subsequence, denoted by the same symbol $\mathbf{E}^0_h$, *converging weakly in* $\mathbf{H}(\mathrm{curl}, \Omega)$ *and strongly in* $\mathbf{L}^2(\Omega)$ *to a divergence-free field* $\mathbf{E} \in \mathbf{H}(\mathrm{curl},\Omega)$.

PROOF. We begin by noticing that the weak convergence is not an issue and, at the cost of replacing the original sequence with an appropriate subsequence, we can assume from the very beginning that the sequence converges weakly to some limit $\mathbf{E}$. The point is to prove the strong $\mathbf{L}^2$-convergence. We begin with a Helmholtz decomposition:

$$\mathbf{E}^0_h = \mathbf{E}^h + \nabla q^h, \tag{3.47}$$

where q^h 'carries' the divergence of $\mathbf{E}^0_h$,

$$\begin{aligned} q^h &\in H^1_0(\Omega), \\ \left(\nabla q^h, \nabla p\right) &= \left(\mathbf{E}^0_h, \nabla p\right), \qquad \forall p \in H^1_0(\Omega), \end{aligned} \tag{3.48}$$

and $\mathbf{E}^h$ is a divergence-free remainder, and therefore, sits in space X_N. Moreover, due to the fact that both $\nabla\mathbf{E}^0_h$ and $\nabla \times \mathbf{E}^0_h$ are constant *elementwise*, gradient $\nabla\mathbf{E}^0_h$ remains bounded[3],

$$\sum_K \left\|\nabla\mathbf{E}^0_h\right\|^2_K \leq C \sum_K \left\|\nabla \times \mathbf{E}^0_h\right\|^2_K \leq C. \tag{3.49}$$

[3]Unfortunately, this elementary argument *does not* apply to rectangular elements.

Consequently, by a standard interpolation result, we can select finite element functions q_h such that

$$\begin{aligned}\left\|\nabla\left(q^h-q_h\right)\right\| &\leq C\left(\sum_K h_K^{1-2\epsilon}\left\|\nabla q^h\right\|^2_{H^{1/2-\epsilon}(K)}\right)^{1/2}\\ &\leq C\left(\sum_K h_K^{1-2\epsilon}\left\|\mathbf{E}_h^0-\mathbf{E}^h\right\|^2_{H^{1/2-\epsilon}(K)}\right)^{1/2}\\ &\leq C\left(\sum_K 2h_K^{1-2\epsilon}\left(\left\|\mathbf{E}_h^0\right\|^2_{H^{1/2-\epsilon}(K)}+\left\|\mathbf{E}^h\right\|^2_{H^{1/2-\epsilon}(K)}\right)\right)^{1/2}\\ &\leq C\left(\sum_K 2h_K^{1-2\epsilon}\left(\left\|\mathbf{E}_h^0\right\|^2_{H^1(K)}+\left\|\mathbf{E}^h\right\|^2_{H^{1/2-\epsilon}(K)}\right)\right)^{1/2}.\end{aligned} \tag{3.50}$$

Now, $\nabla\times\mathbf{E}^h=\nabla\times\mathbf{E}_h^0$, $\nabla\circ\mathbf{E}^h=0$. Consequently, by subadditivity of the $H^{1/2-\epsilon}$-norm (see [21], the real interpolation method) and Theorem 1,

$$\begin{aligned}\sum_K\left\|\mathbf{E}^h\right\|^2_{H^{1/2-\epsilon}(K)} &\leq \left\|\mathbf{E}^h\right\|^2_{H^{1/2-\epsilon}(\Omega)}\\ &\leq C\left\|\nabla\times\mathbf{E}^h\right\|^2=C\left\|\nabla\times\mathbf{E}_h^0\right\|^2\leq C.\end{aligned} \tag{3.51}$$

Also,

$$\begin{aligned}\sum_K\left\|\mathbf{E}_h^0\right\|^2_{H^1(K)} &= \left\|\mathbf{E}_h^0\right\|^2_{L^2(\Omega)}+\sum_K\left\|\nabla\mathbf{E}_h^0\right\|^2_{L^2(K)}\\ &\leq \left\|\mathbf{E}_h^0\right\|^2_{L^2(\Omega)}+C\sum_K\left\|\nabla\times\mathbf{E}_h^0\right\|^2_{L^2(K)}\\ &\leq 1+C.\end{aligned} \tag{3.52}$$

Consequently, $\|\nabla(q^h-q_h)\|$ converges to zero, as maximum element size $h=\max_K h_K$ goes to zero. Notice that we control the regularity of functions $\mathbf{E}_h^0$ *only elementwise*[4], as this is sufficient to establish the estimate for interpolant q_h constructed on the same mesh.

By the compactness argument, at the cost of replacing $\mathbf{E}_h^0$ with a subsequence, denoted by the same symbol, we can assume that $\mathbf{E}^h$ converges to limit $\mathbf{E}$ strongly in $L^2(\Omega)$. It follows from the L^2-convergence that limit $\mathbf{E}$ is divergence-free.

Finally, from the Helmholtz decomposition, and the orthogonality of $\mathbf{E}_h$ to gradients ∇q_h, we have

$$\begin{aligned}\left(\mathbf{E}_h^0,\nabla\left(q^h-q_h\right)\right) &= \left(\mathbf{E}_h^0,\nabla q^h\right)\\ &= \left(\mathbf{E}^h,\nabla q^h\right)+\left(\nabla q^h,\nabla q^h\right)\\ &= \left(\mathbf{E}^h-\mathbf{E},\nabla q^h\right)+\left(\nabla q^h,\nabla q^h\right).\end{aligned} \tag{3.53}$$

This yields the final estimate

$$\left\|\nabla q^h\right\|^2\leq\left\|\mathbf{E}_h\right\|\,\left\|\nabla\left(q^h-q_h\right)\right\|+\left\|\mathbf{E}^h-\mathbf{E}\right\|\,\left\|\nabla q^h\right\|, \tag{3.54}$$

which implies that $\|\nabla q^h\|$ converges to zero. Consequently, $\mathbf{E}$ is the limit of $\mathbf{E}_h^0$ as well. ∎

As noted in the proof, Kikuchi's technique does not generalize to quads. The new result of Boffi [16] providing a link between the discrete compactness and the de Rham diagram properties, will hopefully allow us to cover the case of quadrilateral as well as hybrid, consisting of both quads and triangles, meshes as well. The point we are trying to make here is that, once the discrete compactness property is known for the lowest order elements, it naturally extends (at least in 2D) to elements of an arbitrary and possibly locally variable order.

We begin with a characterization of the elements of higher order.

[4]The normal component of $\mathbf{E}_h^0$, in general, is discontinuous across interelement boundaries.

LEMMA 1. *Let K be an arbitrary triangular or quadrilateral element. Any field $\mathbf{E}_h \in \mathbf{W}_h(K)$ can be represented in the form:*

$$\mathbf{E}_h = \mathbf{E}_h^0 + \nabla\phi_h^e + \mathbf{E}_h^m + \nabla\phi_h^m, \tag{3.55}$$

where

- $\mathbf{E}_h^0$ *is the zero order component such that*

$$\int_e (\mathbf{E}_h - \mathbf{E}_h^0)_t = 0, \tag{3.56}$$

  for each edge e of the element,
- ϕ_h^e *belongs to the span of the mid-edge nodes shape functions,*
- ϕ_h^m *belongs to the span of the middle node shape functions,*
- $\mathbf{E}_h^m$ *belongs to the span of the middle node shape functions and it satisfies the orthogonality condition:*

$$\int_K \mathbf{E}_h^m \nabla q_h^m = 0, \qquad \forall q_h^m. \tag{3.57}$$

PROOF. Condition (3.56) defines uniquely $\mathbf{E}_h^0$. Integrating the tangential component $(\mathbf{E}_h - \mathbf{E}_h^0)_t$ along the boundary ∂K of the element, we can determine a scalar-valued function ϕ_h^e spanned by the mid-edge shape functions such that the tangential component of

$$\mathbf{E}_h - \mathbf{E}_h^0 - \nabla\phi_h^e \tag{3.58}$$

vanishes along boundary ∂K. Consequently, the function belongs to the span of the middle node shape functions. The contribution then can be split into the gradient $\nabla\phi_h^m$ and the orthogonal component $\mathbf{E}_h^m$. ∎

COROLLARY. *Decomposition (3.55) holds for any parametric element K and, consequently, it holds for the whole discrete field $\mathbf{E}_h$ defined on the whole mesh. Field $\mathbf{E}_h^0$ can additionally be split using the discrete Helmholtz decomposition*

$$\mathbf{E}_h^0 = \mathbf{E}_{h0}^0 + \nabla\phi_h^v, \tag{3.59}$$

where function ϕ_h^v belongs to the span of the linear (bilinear for quads) shape functions and $\mathbf{E}_{h0}^0$ is discrete divergence-free, i.e.,

$$(\mathbf{E}_{h0}^0, \nabla q_h^v) = 0, \qquad \forall q_h^v. \tag{3.60}$$

LEMMA 2. *Consider the decomposition*

$$\begin{aligned} \mathbf{E}_h &= \mathbf{E}_h^0 + \nabla\phi_h^e + \mathbf{E}_h^m + \nabla\phi_v^m \\ &= \mathbf{E}_{h0}^0 + \nabla\phi_h^v + \nabla\phi_h^e + \mathbf{E}_h^m + \nabla\phi_h^m. \end{aligned} \tag{3.61}$$

There exists a constant $C > 0$, independent of h, such that

$$\|\nabla \times \mathbf{E}_{h0}^0\| = \|\nabla \times \mathbf{E}_h^0\| \le C\|\nabla \times \mathbf{E}_h\|. \tag{3.62}$$

PROOF. Recall that $\nabla \times \mathbf{E}_h^0$ is constant within each affine element. We have then

$$\begin{aligned} \int_K \nabla \times \mathbf{E}_h^0 &= \int_K \nabla \times (\mathbf{E}_h^0 + \nabla\phi_h^e) \\ &= \int_{\partial K} \mathbf{n} \times (\mathbf{E}_h^0 + \nabla\phi_h^e) \\ &= \int_{\partial K} \nabla \times (\mathbf{E}_h^0 + \nabla\phi_h^e + \nabla\mathbf{E}_h^m + \nabla\phi_h^m) \\ &= \int_K \nabla \times \mathbf{E}_h. \end{aligned} \tag{3.63}$$

Consequently, for shape regular elements, there exists a constant C such that

$$\begin{aligned}\int_K \left|\nabla \times \mathbf{E}_h^0\right|^2 &\leq Ch^2 \left|\nabla \times \mathbf{E}_h^0\right|^2 \\ &\leq \frac{C}{h^2}\left(\int_K \left|\nabla \times \mathbf{E}_h^0\right|\right)^2 = \frac{C}{h^2}\left|\int_K \nabla \times \mathbf{E}_h^0\right|^2 \\ &= \frac{C}{h^2}\left|\int_K \nabla \times \mathbf{E}_h\right|^2 \\ &\leq C\int_K |\nabla \times \mathbf{E}_h|^2. \end{aligned} \tag{3.64}$$

∎

LEMMA 3. *Let K be an arbitrary element and let $\mathbf{E}_h^m$ denote an arbitrary combination of the middle node shape functions as in (3.55), satisfying orthogonality condition (3.57). Then there exists a constant $C > 0$ such that*

$$\int_K |\mathbf{E}_h^m|^2 \leq Ch^2 \int_K |\nabla \times \mathbf{E}_h^m|^2. \tag{3.65}$$

PROOF. Both sides of (3.65) define a norm on the space of the middle node shape functions satisfying the orthogonality condition. Thus, by equivalence of norms on finite dimensional spaces, the inequality holds on the master element with $h = 1$ and some constant C. The result for an arbitrary element follows then from the usual scaling argument. ∎

We are able now to state and prove our main result.

THEOREM 3. *Let $\mathbf{E}_h \in \mathbf{W}_h$ be a sequence of fields corresponding to the hp elements discussed earlier with possibly variable but limited order of approximation $p \leq p_0$. Assume that*

- *$\mathbf{E}_h$ is uniformly bounded in the $\mathbf{H}(\mathrm{curl}, \Omega)$-norm,*

$$\|\mathbf{E}_h\|^2 + \|\nabla \times \mathbf{E}_h\|^2 \leq 1, \qquad \forall h; \tag{3.66}$$

- *$\mathbf{E}_h$ are discrete divergence-free,*

$$(\mathbf{E}_h, \nabla q_h) = 0, \qquad \forall q_h \in V_h. \tag{3.67}$$

Then there exists a subsequence $\mathbf{E}_h$ (denoted for simplicity with the same symbol) converging weakly in $\mathbf{H}(\mathrm{curl}, \Omega)$, and strongly in $\mathbf{L}^2(\Omega)$ to a divergence-free function $\mathbf{E} \in \mathbf{H}(\mathrm{curl}, \Omega)$.

PROOF. The same way as in Theorem 2, the weak convergence is not an issue, and the point is to prove the strong $\mathbf{L}^2$-convergence.

Step 1. By Theorem 2, the smallest positive approximate eigenvalue $\lambda_h^1 > 0$ corresponding to the 0^{th}-order elements approximation, converges to its exact counterpart $\lambda_1 > 0$. Thus, $(\lambda_h^1)^{-1}$ must be bounded by a constant C. We can then bound the $\mathbf{L}^2$-norm of the $\mathbf{E}_{h0}^0$-component by the L^2-norm of its curl, and in turn, by Lemma 1, by the L^2-norm of the curl of the total field

$$\left\|\mathbf{E}_{h0}^0\right\| \leq \left(\lambda_h^1\right)^{-1} \left\|\nabla \times \mathbf{E}_{h0}^0\right\| \leq C\left\|\nabla \times \mathbf{E}_h^0\right\| \leq C\|\nabla \times \mathbf{E}_h\|. \tag{3.68}$$

Step 2. Consequently, $\mathbf{E}_{h0}^0$ satisfies the assumptions of Theorem 1, and we can extract a subsequence $\mathbf{E}_{h0}^0$ converging weakly in $\mathbf{H}(\mathrm{curl}, \Omega)$ and strongly in $\mathbf{L}^2(\Omega)$ to a divergence-free limit $\mathbf{E}^0$.

Step 3. Denote

$$\phi_h = \phi_h^v + \phi_h^e + \phi_h^m. \tag{3.69}$$

We have:

$$\begin{aligned}(\nabla\phi_h, \nabla\phi_h) &= -\left(\mathbf{E}_{h0}^0 + \mathbf{E}_h^m, \nabla\phi_h\right) \\ &= \left(\mathbf{E}^0 - \mathbf{E}_{h0}^0 - \mathbf{E}_h^m, \nabla\phi_h\right),\end{aligned} \tag{3.70}$$

since $\mathbf{E}^0$ is divergence-free. Consequently,

$$\|\nabla\phi_h\| \leq \left\|\mathbf{E}^0 - \mathbf{E}_{h0}^0\right\| + \|\mathbf{E}_h^m\|. \tag{3.71}$$

Step 4. By the scaling argument from Lemma 3 and the Lemma 2 result,

$$\begin{aligned}\|\mathbf{E}_h^m\|^2 &\leq Ch^2 \sum_K \|\nabla \times \mathbf{E}_h^m\|_K^2 \\ &\leq Ch^2 \sum_K \left\|\nabla \times \left(\mathbf{E}_h - \mathbf{E}_h^0\right)\right\|_K^2 \\ &\leq Ch^2 \sum_K \|\nabla \times \mathbf{E}_h\|^2 \leq Ch^2.\end{aligned} \tag{3.72}$$

Thus, $\|\mathbf{E}_h^m\| \to 0$, and therefore, $\|\nabla\phi_h\| \to 0$ as well. This implies that $\mathbf{E}_h$ converges strongly in $\mathbf{L}^2(\Omega)$ to $\mathbf{E} = \mathbf{E}^0$.

4. NUMERICAL EXPERIMENTS

The presented theory is tested on two computational domains with perfect electric conductor (PEC) boundary conditions: $3\pi/2$-sector of a unit radius, see Figure 4, and a unit circle with a slit, see Figure 5.

For these domains, analytical solutions can be constructed by using the procedure outlined below. In two dimensions, any divergence-free field can be represented as the curl of a scalar-valued function. In order to satisfy PEC boundary conditions, Neumann boundary conditions should be imposed on the function. The curl-curl operator acts on scalar functions as the Laplace operator, and therefore, the eigenfields of the curl-curl operator can be computed by taking the curl of the eigenfunctions for the Laplace operator with Neumann boundary conditions. The eigenvalues remain unchanged.

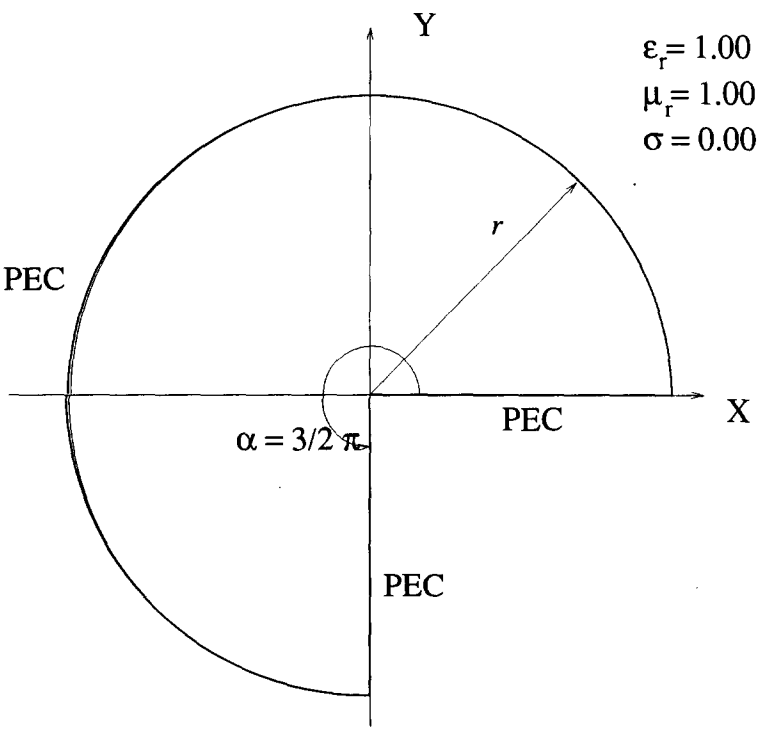

Figure 4. Sector domain.

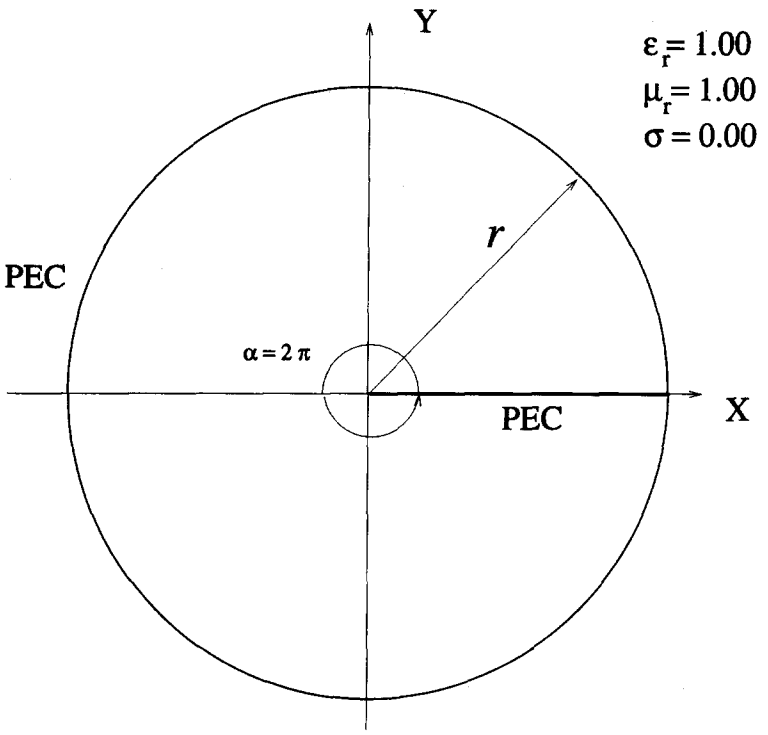

Figure 5. Slit domain.

The eigenvalue problem for the Laplace operator in a sector of angle α and radius r:

$$\begin{aligned} -\nabla^2 f &= \lambda^2 f, && \text{in } \Omega, \\ \frac{\partial f}{\partial n} &= 0, && \text{on } \partial\Omega \end{aligned} \tag{4.73}$$

can be solved analytically to yield the following eigenpairs $(\lambda^2{}_{nk}, f_{nk})$:

$$\begin{aligned} f_{nk}(\rho,\theta) &= J_{\pi n/\alpha}(\lambda_{nk}\rho)\cos\left(\frac{\pi n}{\alpha}\theta\right), && n = 0,1,2,\ldots, \\ \frac{d}{d\rho}\left(J_{\pi n/\alpha}(\lambda_{nk}\rho)\right)|_{\rho=r} &= 0, && \text{solve for } \lambda_{nk},\ n \text{ is fixed.} \end{aligned} \tag{4.74}$$

The eigenfields corresponding to the first four eigenvalues follow:

- for domain in Figure 4,

$$\mathbf{E}_n(\rho,\theta) = \nabla \times \left(J_{2n/3}(\lambda_n\rho)\cos\left(\frac{2n}{3}\theta\right)\right), \qquad n = 1,2,3,4.$$

- for domain in Figure 5,

$$\mathbf{E}_n(\rho,\theta) = \nabla \times \left(J_{n/2}(\lambda_n\rho)\cos\left(\frac{n}{2}\theta\right)\right), \qquad n = 1,2,3,4. \tag{4.75}$$

The first four eigenvalues considered to be "exact" have been calculated from equation (4.73.2) using MAPLE.

Table 1.

Sector	Slit
1.4617041754176002 E + 01	9.328363212358877 E + 00
9.3283636521690010 E + 00	6.054235301077367 E + 00
5.0974576400249996 E + 00	3.389957715417456 E + 00
1.9634118835240002 E + 00	1.358532875978604 E + 00

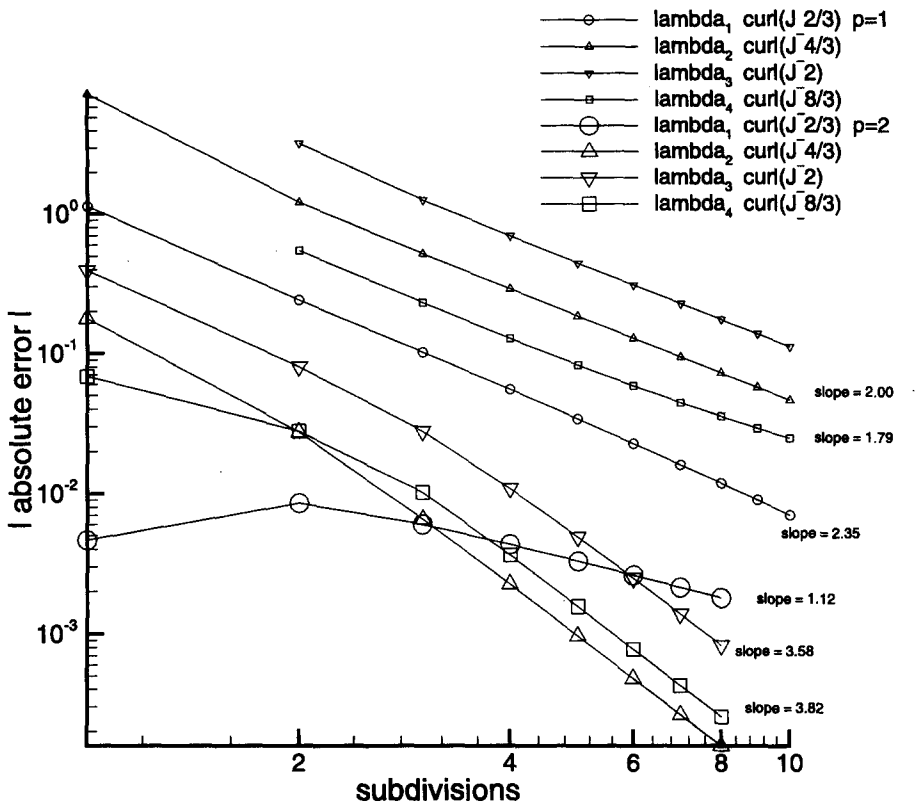

Figure 6. Sector domain: convergence plots for the first four eigenvalues.

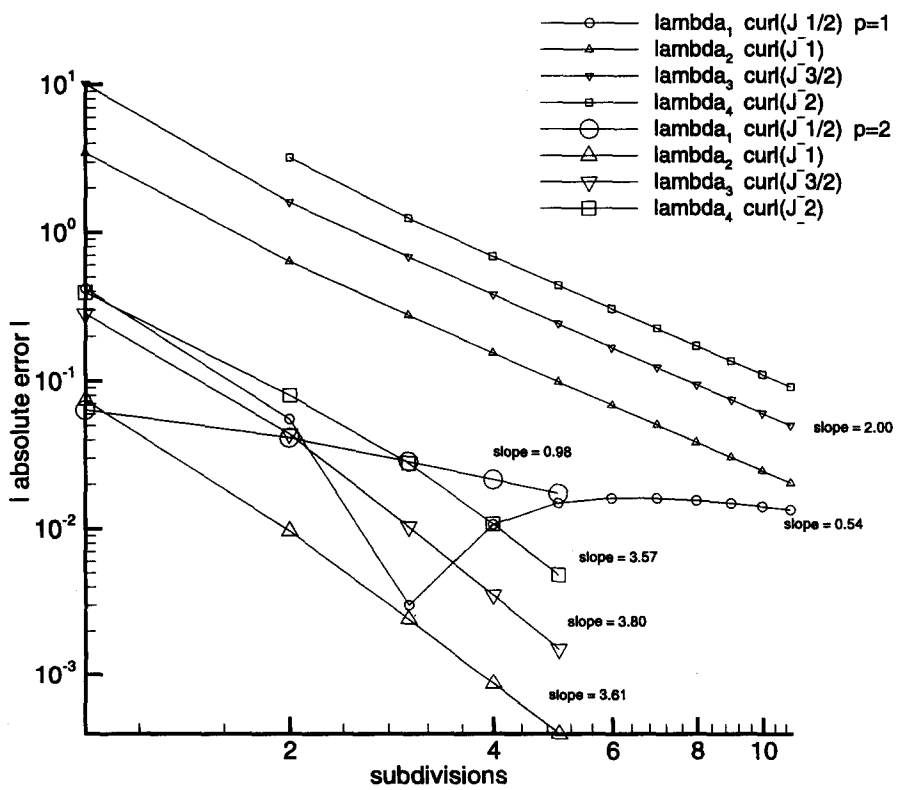

Figure 7. Slit domain: convergence plots for the first four eigenvalues.

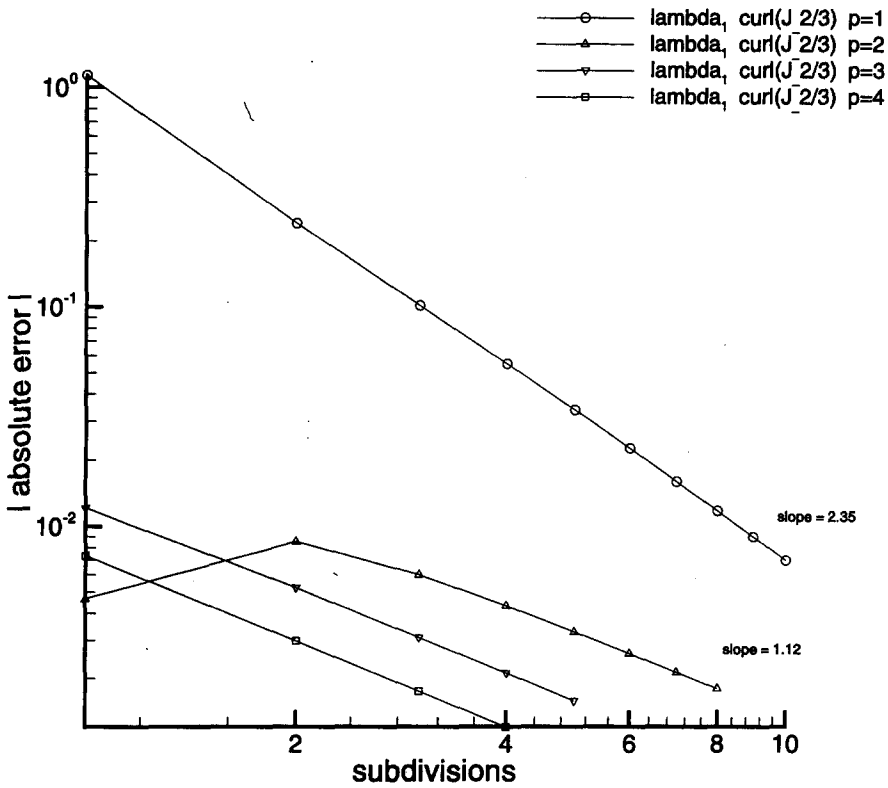

Figure 8. Sector domain: convergence plots for the first eigenvalue, for $p = 1, 2, 3$.

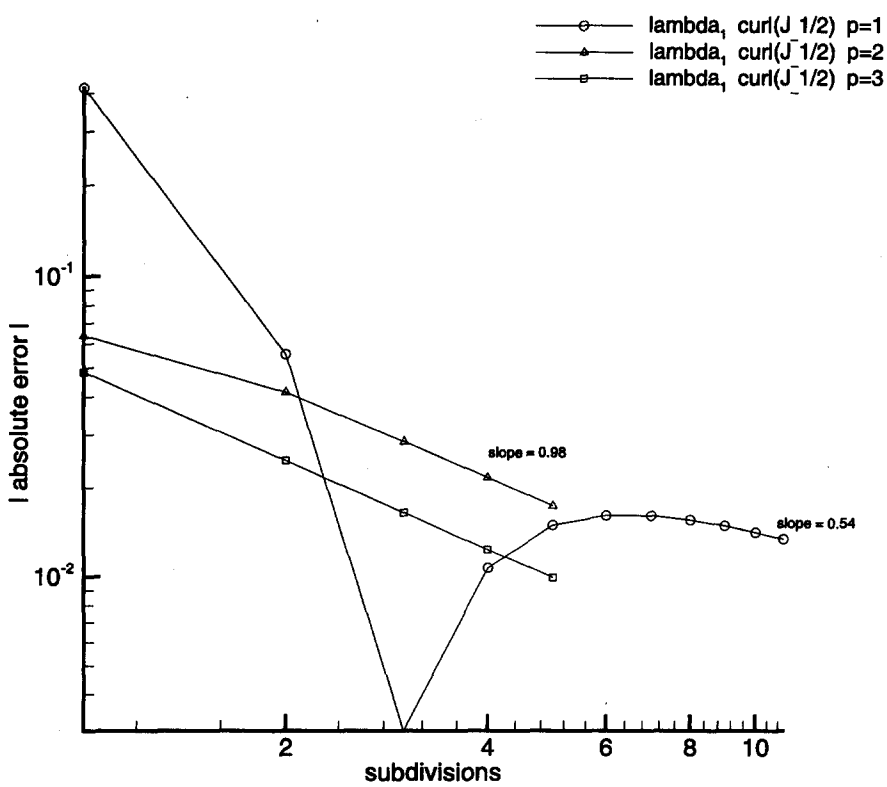

Figure 9. Slit domain: convergence plots for the first eigenvalue, for $p = 1, 2, 3$.

The "approximate" eigenvalues are produced by the DGEGV routine of LAPACK interfaced with 2Dhp90_EM, the finite element code described in [14].

The plots in Figure 6 and Figure 7 demonstrate the convergence rates for uniform h-refinements with element order ranging from 1 to 4 for the sector, and from 1 to 3 for the slit domain. The initial mesh consists of three triangular elements for the sector, and of four elements for the slit domain. In the course of experiments, each element is subdivided up to 11 times in each direction.

The plots in Figure 8 and Figure 9 show the rate of convergence for the smallest eigenvalue for each domain. For either domain, the smallest eigenvalue corresponds to a singular eigenfield. The graph of the error for the smallest eigenvalue in the slit domain exhibits a sudden rise after a dramatic fall when the number of subdivisions is changed from 3 to 4. Initially, the computed eigenvalue approaches the "exact" one from above, but after the third subdivision, the computed eigenvalue remains below the "exact" one. The understanding of this phenomenon is a subject of a further investigation.

We conclude by stating that the graphs confirm, even for the "worst" possible case in two dimensions, the h-convergence of the eigenvalues for the FE approximation of the curl-curl operator. This, in particular, guarantees stability and convergence of the FE approximations to time-harmonic Maxwell's equations [1,6].

REFERENCES

1. L. Demkowicz and L. Vardapetyan, Modeling of electromagnetic absoption/scattering problems using *hp*-adaptive finite elements, *Computer Methods in Applied Mechanics and Engineering* **152** (1/2), 103-124, (1998).
2. L. Vardapetyan and L. Demkowicz, *hp*-adaptive finite elements in electromagnetics, *Computers Methods in Applied Mechanics and Engineering* **169**, 331–344, (1999).
3. D. Boffi, Discrete compactness and Fortin operator for edge elements, Preprint, (March 1999).
4. F. Kikuchi, Mixed and penalty formulations for finite element analysis of an eigenvalue problem in electromagnetism, *Computer Methods in Applied Mechanics and Engineering* **64**, 509–521, (1987).
5. F. Kikuchi, On a discrete compactness property for the Nedelec finite elements, *J. Fac. Sci. Univ. Tokyo, Sect. IA, Math.* **36**, 479–490, (1989).
6. P. Monk, L. Demkowicz and L. Vardapetyan, Discrete compactness and the approximation of Maxwell's equations in $\mathbb{R}^3$, Preprint, (October 1998).
7. V. Levillain, Eigenvalue approximation by mixed methods for resonant inhomogeneous cavities with metallic boundaries, *Mathematics of Computation* **58**, 11–20, (1992).
8. P. Joly, C. Poirier, J. Roberts and P. Trouve, A new nonconforming finite element method for the computation of electromagnetic guided waves 1: Mathematical analysis, *SIAM J. Numer. Anal.* **33**, 1494–1525, (1996).
9. R. Leis, *Initial Boundary Value Problems in Mathematical Physics*, Teubner, (1986).
10. M. Cessenat, *Mathematical Methods in Electromagnetism, Linear Theory and Applications*, World Scientific, London, (1996).
11. M. Costabel and M. Dauge, Singularities of electromagnetic fields in polyhedral domains, Technical Report 98-24, Report available at `http://www.maths.univ-rennes1.fr/~costabel/`, IRMAR, Université de Rennes 1, France, (1998).
12. J.C. Nedelec, Mixed finite elements in $\mathbb{R}^3$, *Numerische Mathematik* **35**, 315–341, (1980).
13. J.C. Nedelec, A new family of mixed finite elements in $\mathbb{R}^3$, *Numerische Mathematik* **50**, 57–81, (1986).
14. W. Rachowicz and L. Demkowicz, A two-dimensional *hp*-adaptive finite element package for electromagnetics, TICAM Report 98-15, July 1998; *Computer Methods in Applied Mechanics and Engineering* (to appear).
15. B. Mercier, J. Osborn, J. Rappaz and P.A. Raviart, Eigenvalue approximation by mixed and hybrid methods, *Mathematics of Computation* **36**, 427–453, (1981).
16. D. Boffi, A note on the discrete compactness property and the de Rham diagram, Preprint, (April 1999).
17. L. Demkowicz, P. Monk, L. Vardapetyan and W. Rachowicz, De Rham diagram for *hp* finite element spaces, TICAM Report 99-06, (March 1999).
18. A. Bermudez and D.G. Pedreira, Mathematical analysis of a finite element method without spurious solutions for computation of dielectric wavequides, *Numerische Mathematik* **61**, 39–57, (1992).
19. L. Demkowicz, T. Walsh, K. Gerdes and A. Bajer, 2D *hp*-adaptive finite element package. Fortran 90 implementation (2Dhp90), TICAM Report 98-14, The University of Texas at Austin, Austin, TX 78712.
20. M. Costabel and M. Dauge, Singularities of Maxwell's equations on polyhedral domains, Prepublication 96-30, IRMAR, Université de Rennes 1, France, (October 1996).
21. J. Bergh and J. Löfstrom, *Interpolation Spaces, An Introduction*, Springer-Verlag, Berlin, (1976).